IN-FLIGHT COMPRESSIBLE TURBULENT BOUNDARY LAYER MEASUREMENTS ON A HOLLOW CYLINDER AT A MACH NUMBER OF 3.0

Robert D. Quinn and Leslie Gong
Dryden Flight Research Center

SUMMARY

Skin temperatures, shearing forces, surface static pressures, and boundary layer pitot pressures and total temperatures were measured on a hollow cylinder 3.04 meters long and 0.437 meter in diameter mounted beneath the fuselage of the YF-12A airplane. The data were obtained at a nominal free stream Mach number of 3.0 and at wall-to-recovery temperature ratios of 0.66 to 0.91. The free stream Reynolds number had a nominal value of 4.2×10^6 per meter. Heat transfer coefficients and skin friction coefficients were derived from skin temperature time histories and shear force measurements, respectively. Also, boundary layer velocity profiles were derived from pitot pressure measurements, and a Reynolds analogy factor of 1.11 was obtained from the measured heat transfer and skin friction data.

Skin friction, calculated by the theory of van Driest, by Eckert's reference enthalpy method, and by the Spalding and Chi method, was compared with the measured data. The skin friction coefficients predicted by the theory of van Driest were in excellent agreement with the measurements. Theoretical heat transfer coefficients, in the form of Stanton numbers calculated by using a modified Reynolds analogy between skin friction and heat transfer, were compared with measured values. The theory of van Driest, together with the experimentally determined Reynolds analogy factor of 1.11, predicted heat transfer coefficients that were in excellent agreement with the measured data. The measured velocity profiles were compared to Coles' incompressible law-of-the-wall profile by transforming the compressible measured data to their incompressible values. The transformation methods of van Driest and Eckert both gave good correlation.

INTRODUCTION

Accurate calculations of turbulent skin friction and heat transfer are required

for the efficient and safe design of high-speed aircraft. A large number of empirical and semiempirical theories are available which can be used to predict skin friction and heat transfer. However, values predicted by the various theories usually differ substantially; therefore, experiments must be performed to determine the validity of the theories. A large amount of experimental skin friction and heat transfer data has been obtained in the wind tunnel (refs. 1 and 2). Unfortunately, the wind tunnel tests have shown conflicting results (refs. 3 and 4). Data obtained from flight have also differed from the wind tunnel results (refs. 5 and 6). This lack of agreement in results obtained from the various experimental tests has hampered the evaluation of turbulent boundary layer theories and clearly indicates the need for further study.

The YF-12A airplane with its Mach 3 cruise capability offered an excellent test bed for compressible turbulent boundary layer measurements. Consequently, an instrumented hollow cylinder 3.04 meters in length was installed beneath the fuselage of the YF-12A airplane to obtain flight-measured turbulent boundary layer data that could be used to evaluate the various turbulent predicting methods. In addition, the size of the hollow cylinder would allow the same cylinder with the same instrumentation to be tested in the wind tunnel so that flight and wind tunnel measurements could be directly compared.

This paper presents flight data that were obtained on a hollow cylinder during two YF-12 flights designated flights A and B. During flight A, skin friction and boundary layer profile data were obtained at a local Mach number of 2.9, at a wall-to-recovery temperature ratio of 0.91, and at a momentum thickness Reynolds number of 8664. During flight B, heat transfer and skin friction data were obtained at a local Mach number of 2.92, at wall-to-recovery temperatures of 0.66 to 0.71 and at a local Reynolds number of 4.17×10^6 per meter. The measured data are compared to values calculated by various predicting methods. In addition, boundary layer transition determined from measured temperatures and measured heat transfer are presented.

SYMBOLS

Physical quantities in this report are given in the International System of Units (SI).

C_f local skin friction coefficient

Fc transformation function for skin friction, $\frac{\bar{C}_f}{C_f}$

Fx transformation function for length Reynolds number, $\frac{\bar{Re}_x}{Re_x}$ or $\frac{\bar{Re}_L}{Re_L}$

h	altitude, m
h_H	local heat transfer coefficient based on enthalpy, kg/m^2-sec
L	length of turbulent flow, m
M	Mach number
P	pressure, N/m^2
Re	unit Reynolds number, $\frac{\rho U}{\mu}$, m^{-1}
Re_L	Reynolds number based on length of turbulent boundary layer flow, $\frac{\rho_\delta U_\delta L}{\mu_\delta}$
Re_x	Reynolds number based on distance from the leading edge, $\frac{\rho_\delta U_\delta x}{\mu_\delta}$
Re_θ	Reynolds number based on momentum thickness, $\frac{\rho_\delta U_\delta \theta}{\mu_\delta}$
St	local Stanton number, $\frac{h_H}{\rho_\delta U_\delta}$
s	Reynolds analogy factor
T	temperature, K
T_R	boundary layer recovery temperature, K
U	velocity, m/sec
U_τ	friction velocity, $\sqrt{\frac{\tau}{\rho}}$
x	distance from leading edge, m
y	distance normal to surface of cylinder, cm
α	angle of attack, deg
β	angle of sideslip, deg
δ	total boundary layer thickness, cm

θ	boundary layer momentum thickness, cm
μ	dynamic viscosity, N-sec/m^2
ν	kinematic viscosity, m^2/sec
ρ	density of air, kg/m^3
τ	shearing stress, N/m^2

Subscripts:

t	total conditions
w	wall or skin
δ	boundary layer edge conditions
∞	free stream

Superscripts:

$(\bar{})$	incompressible variable or a variable that has been transformed to the equivalent constant property case

DESCRIPTION OF EQUIPMENT

A hollow cylinder, 3.04 meters in length and 0.437 meter in outside diameter, was installed on the lower fuselage of the YF-12A airplane, as shown in figure 1. The cylinder was attached to a pylon which was mounted to hard points on the aircraft. The pylon provided a vertical separation distance of 0.46 meter between the aircraft fuselage and the hollow cylinder. A photograph of the airplane with the cylinder installed is shown in figure 2. The cylinder skin was 0.127 centimeter thick and had a sharp leading edge with a radius of 0.0127 centimeter. A complete description of the airplane can be found in reference 7.

INSTRUMENTATION

As shown in figure 3, the cylinder was instrumented with 123 thermocouples, 34 static pressure orifices, a skin friction balance, a pitot pressure rake, and a total temperature boundary-layer rake. The thermocouples were 30-gage chromel-alumel wires spot welded to the inside surface of the skin. The pressure orifices were tubing with an inside diameter of 0.32 centimeter installed flush with the outside surface of the skin. The skin friction gage was a commercially developed, liquid-cooled force balance installed flush with the surface of the cylinder at the location shown in figure 3. A detailed description of the skin friction gage is given in reference 8. The pitot pressure rake and the total temperature rake were installed

274.12 centimeters aft of the leading edge, and, as shown in figure 3, the pitot pressure rake was installed on the lower surface centerline and the total temperature rake was located on the lower surface at an angular displacement of 16.25° from the vertical centerline. The outermost probe on the pressure rake was a 20° half angle conical probe used to measure flow angles needed to insure that the cylinder was aligned with the local flow.

The primary boundary layer measurements were made on the lower centerline of the cylinder. Data presented in this paper were obtained from these measurements. The surface static pressure measurements and the skin temperature measurements made at the other locations were used to detect any anomalies in the flow field on the cylinder.

TEST CONDITIONS

In order to obtain meaningful boundary layer measurements, the hollow cylinder had to be installed at a location on the YF-12A airplane where the local flow was uniform. Consequently, before the aircraft installation was made, flow-field surveys were conducted on a 1/25-scale model of the YF-12A airplane in the Langley Unitary Plan Wind Tunnel (ref. 9) and on the YF-12A airplane in flight. These tests confirmed that the local flow field below the airplane was uniform in the area where the cylinder was to be located.

Two configurations of the cylinder were used in the experiment. The first configuration, tested during flight A, is shown in figure 4. With this configuration the wall or skin temperature is always at or near radiation equilibrium temperature and, consequently, heat transfer data were not obtained during flight A. The second configuration, tested during flight B, is shown in figure 5. In this configuration the cylinder was insulated with a frangible cover which was used to provide low initial wall temperatures. Prior to takeoff, to insure that the measurements were obtained at cold surface temperatures, the cylinder was cooled to a temperature of 211 K using gaseous nitrogen. When the airplane reached the desired test conditions, the insulation was removed within 50 milliseconds and the test data were obtained.

Time histories of free stream Mach number, altitude, and angle of attack for flights A and B are shown in figures 6(a) and 6(b), respectively. Also shown in each figure is a typical skin-temperature time history. The shaded portion of these flight profiles indicates the time during which the boundary layer data of this experiment were obtained. Also shown in figure 6(b) is the time at which the insulation was removed. As can be seen, once the insulation was removed, the skin temperature increased at a rapid rate. It was during this period of high heating rates that the heat transfer and other boundary layer data were obtained. The free stream conditions at which the data presented in this paper were obtained are given in table 1. The local (cylinder) test conditions at which the data were obtained are given in table 2.

It should be noted that the boundary layer edge static pressure given in table 2 was actually measured on the surface of the cylinder. The usual assumption was made that the static pressure through the boundary layer was constant. Also, the wall-to-recovery temperature ratio given in table 2 for flight A is based on the wall

temperature measured on the lower centerline of the cylinder at the skin friction balance location, and is slightly lower than the wall-to-recovery temperature ratios on the cylinder forward of this location.

RESULTS AND DISCUSSION

Surface Static Pressures

The surface static pressures measured on the lower centerline of the cylinder are shown in figure 7. Figure 7(a) shows the data obtained during flight A, and figure 7(b) shows the data obtained during flight B. The solid lines in these figures are straight line fairings of the data. The pressures were constant and equal to 4943 N/m^2 for flight A and 4413 N/m^2 for flight B.

Boundary Layer Profiles

The Mach number and velocity profiles derived from the data measured during flight A are tabulated in table 3. Also given in table 3 are the boundary layer temperature distribution, the momentum thickness, and the pertinent boundary layer edge conditions. As previously noted, boundary layer profiles were not obtained during flight B.

Measured total temperature ratios obtained during flight A are plotted in figure 8 as a function of the velocity ratio squared. Also shown for comparison purposes is the quadratic profile calculated by the method given in reference 3. The figure shows that the measured data are in excellent agreement with the quadratic distribution.

The boundary layer velocity distribution, calculated from the measured data obtained during flight A, is presented in figure 9. Also shown is the velocity profile predicted by the power law. When a power law exponent of 8 was used, excellent agreement was obtained between the power law velocity profile and the measured data.

Boundary Layer Thickness

A problem often encountered when trying to evaluate the various turbulent skin friction and heat transfer theories is that of determining the virtual origin of turbulent flow. Unless turbulent flow originates at or near the leading edge of the test specimen, the determination of the virtual origin is somewhat arbitrary. This problem can be eliminated if the comparisons of measured data with calculated data are based on momentum thickness Reynolds number. Consequently, one of the primary purposes of the boundary layer surveys was to determine the momentum thickness. However, in order to evaluate the momentum thickness, the total thickness must be determined. In the present investigation the total boundary layer thickness was computed by the method developed in reference 10, which yielded a thickness value of 3.05 centimeters.

Law-of-the-Wall Velocity Profiles

The use of the Clauser technique to obtain skin friction from velocity profiles is well known and is described in reference 11. However, when applying this technique, especially to compressible turbulent boundary layers, there is the inherent problem that the accuracy of the skin friction obtained by this procedure depends on the accuracy of the compressible theory used to predict the law-of-the-wall velocity profile. Therefore, before accurate skin friction can be obtained from velocity profiles, the accuracy of the various theories must be determined.

Comparison of measured and calculated law-of-the-wall velocity profiles are shown in figures 10(a) to 10(c). The solid curve in these figures represents Coles' incompressible values as given in reference 12. The flight data in these figures are the measured compressible boundary layer velocities that have been reduced to their incompressible values by the indicated theory using the shearing stress that was measured by the skin friction balance. In this form the data should agree with the solid line if the theory used to transform the data is correct. The three transformation methods used are the theory of van Driest (ref. 13) shown in figure 10(a), the reference enthalpy method of Eckert (ref. 14), shown in figure 10(b), and the wall reference temperature method as applied in reference 15, shown in figure 10(c). Both the theory of van Driest and Eckert's reference enthalpy method yield good correlation between the measured profiles and Coles' incompressible curve. However, as shown in figure 10(c), the data transformed by the wall reference temperature method are in poor agreement with the incompressible curve.

SKIN FRICTION

Skin friction data were obtained directly from the skin friction balance measurements during flights A and B and indirectly from heat transfer measurements obtained during flight B. The measured skin friction data in the form of shearing force, obtained during flight A, are shown in figure 11. Also shown for comparison and evaluation are the values predicted by the theory of van Driest (ref. 16), the Spalding and Chi method (ref. 17), and Eckert's reference enthalpy method (ref. 14). Values predicted by the theory of van Driest and the method of Spalding and Chi are in excellent agreement with the measured data. However, Eckert's reference enthalpy method underpredicts the measured data by approximately 10 percent.

Origin of turbulence.—All of the calculated values shown in figure 11 were based on momentum thickness Reynolds number. However, because the momentum thickness was not available for the test conditions of flight B, the virtual origin of turbulent flow had to be determined in order to correlate and compare the measured skin friction coefficients obtained from both flights A and B with theoretical predicted values. The first step in determining the virtual origin was to look at the boundary layer transition. If the transition data showed that turbulent flow existed at or near the leading edge of the test specimen, then there was no need to determine a virtual origin because, in this case, the virtual origin could be assumed to be the leading edge.

Figures 12 and 13 show boundary layer transition data obtained on the lower centerline of the cylinder during flights A and B, respectively. In figure 12 the transition data are shown in the form of measured wall temperature as a function of distance from the leading edge. As shown, the beginning of transition occurs at a distance of 0.76 meter and a Reynolds number of 3.4 million, and the end of transition occurs at approximately 1.22 meters and a Reynolds number of 5.5 million. It is obvious from this data that the leading edge is not the origin of turbulent flow and a virtual origin must be determined. Fortunately, the momentum thickness Reynolds number is known for flight A. Consequently, equivalent length Reynolds numbers were determined for each theory that yielded the same results as obtained when using the momentum thickness Reynolds number. The distance from the leading edge determined from these equivalent Reynolds numbers was interpreted as being the virtual origin for the particular theory used. The virtual origins obtained by this procedure are shown in figure 12. Figure 13 shows transition data obtained during flight B. The data are in the form of heat transfer coefficients as a function of distance from the leading edge. It is obvious from these data that transition occurs so close to the leading edge that turbulent flow can be assumed to exist from the leading edge.[1] Consequently, for flight B the length of turbulent flow, L, and the distance from the leading edge, x, are considered to be equal.

Evaluation of compressible transformation theories.—Comparison between measured skin friction coefficients and values predicted by Eckert's reference enthalpy method, the Spalding and Chi method, and the theory of van Driest are shown in figures 14(a), 14(b), and 14(c), respectively. The solid line in these figures represents the incompressible skin friction coefficients predicted by the von Kármán-Schoenherr equation, and the symbols represent the measured data that have been transformed to their incompressible values by the indicated compressible theory. In this form the transformed measured data should agree with the solid line if the theory used to transform the data is correct. The open symbols in figure 14 represent skin friction coefficients that were obtained from the measured heat transfer data using the experimentally determined Reynolds analogy factor of 1.11. The procedure used to determine the experimental Reynolds analogy factor is discussed in the following section of this report. The solid circle symbol represents the skin friction coefficients obtained from the skin friction balance measurements during flight B, and the solid square symbol represents the skin friction balance data obtained during flight A. As can be seen, all three theories do a good job of correlating the skin friction coefficients with Reynolds number. However, the level of skin friction predicted by each transformation theory differs substantially. As can be seen in figure 14(a), the data transformed by Eckert's reference enthalpy method are approximately 10 percent higher than the von Kármán-Schoenherr curve, and this is considered to be fair agreement. Figure 14(b) shows that the measured data are about 7 percent higher than the incompressible values when the Spalding and Chi method is used to transform the data. The agreement shown in this figure is considered to be good. However, as shown in figure 14(c), the measured data transformed by the theory

[1] The fact that the boundary layer transition occurred much closer to the leading edge during flight B than during flight A was not expected, since it is normally assumed that the boundary layer becomes more stable at the lower wall temperatures. The reason for the early transition during flight B has not been determined at this time.

of van Driest are within ±2 percent of the von Kármán-Schoenherr incompressible values and the agreement is considered to be excellent.

Reynolds Analogy Factor

Most turbulent heat transfer methods are based on some form of Reynolds analogy between skin friction and heat transfer. Consequently, once a skin friction equation is selected, a Reynolds analogy factor is needed to calculate heat transfer coefficients. The determination of a Reynolds analogy factor has been the subject of considerable investigation but has still not been resolved (ref. 18). Therefore, heat transfer and skin friction were measured simultaneously during this investigation, and by using the relationship $s = 2St/C_f$, an experimental Reynolds analogy factor was determined, thus eliminating the necessity of estimating a Reynolds analogy factor when making the heat transfer calculation. The Reynolds analogy factor determined from the measured skin friction and heat transfer was 1.11.

Heat Transfer

Figure 15 shows the comparison between the measured heat transfer coefficients, in the form of Stanton numbers, and the theoretical values predicted by the theory of van Driest using an experimental Reynolds analogy factor of 1.11. The dashed line represents the laminar Stanton numbers predicted by Eckert's reference enthalpy method. The values predicted by the theory of van Driest are represented by two solid lines. The upper line represents the Stanton numbers that were calculated using a wall-to-recovery temperature ratio of 0.66 and the lower line represents values computed using a temperature ratio of 0.71. As shown, the Stanton numbers predicted by the theory of van Driest are in excellent agreement with the measured heat transfer data.

CONCLUSIONS

Flight-measured turbulent skin friction, heat transfer, and boundary layer velocity profiles were measured on the lower centerline of a hollow cylinder 3.04 meters in length at a nominal free stream Mach number of 3.0, at wall-to-recovery temperature ratios of 0.66 to 0.91 and at local Reynolds numbers of 1 to 12 million. Skin friction coefficients were obtained directly from measurements made by a skin friction force balance and indirectly from heat transfer measurements using a Reynolds analogy factor derived from the force balance and heat transfer data. The results of this investigation led to the following conclusions:

1. The theory of van Driest predicted skin friction coefficients that were in excellent (±2 percent) agreement with the measured data. The Spalding and Chi method predicted skin friction coefficients that were 7 percent lower than the measured coefficients, and the values predicted by Eckert's reference enthalpy method were 10 percent lower than the measured skin friction coefficients.

2. A measured Reynolds analogy factor of 1.11 was derived from the skin friction and heat transfer data.

3. Heat transfer coefficients predicted by the theory of van Driest, using the measured Reynolds analogy factor, were in excellent agreement with the measured heat transfer coefficients.

4. Measured velocity profiles transformed by the theory of van Driest and Eckert's reference enthalpy method were in good agreement with Coles' incompressible law-of-the-wall velocity profile.

REFERENCES

1. Hopkins, Edward J.; Rubesen, Morris W.; Inouye, Mamou; Keener, Earl R.; Mateer, George C.; and Polek, Thomas E.: Summary and Correlation of Skin-Friction and Heat-Transfer Data for a Hypersonic Turbulent Boundary Layer on Simple Shapes. NASA TN D-5089, 1969.

2. Peterson, John B., Jr.: A Comparison of Experimental and Theoretical Results for the Compressible Turbulent-Boundary-Layer Skin Friction With Zero Pressure Gradient. NASA TN D-1795, 1963.

3. Samuels, Richard D.; Peterson, John B., Jr.; and Adcock, Jerry B.: Experimental Investigation of the Turbulent Boundary Layer at a Mach Number of 6 With Heat Transfer at High Reynolds Numbers. NASA TN D-3856, 1967.

4. Hopkins, Edward J.; Keener, Earl R.; and Louie, Pearl T.: Direct Measurements of Turbulent Skin Friction on a Nonadiabatic Flat Plate at Mach Number 6.5 and Comparison With Eight Theories. NASA TN D-5675, 1970.

5. Quinn, Robert D.; and Olinger, Frank V.: Heat-Transfer Measurements Obtained on the X-15 Airplane Including Correlation With Wind-Tunnel Results. NASA TM X-1705, 1969.

6. Banner, Richard D.; Kuhl, Albert E.; and Quinn, Robert D.: Preliminary Results of Aerodynamic Heating Studies on the X-15 Airplane. NASA TM X-638, 1962.

7. NASA YF-12 Flight Loads Program. NASA TM X-3061, 1974.

8. Garringer, Darwin J.; and Saltzman, Edwin J.: Flight Demonstration of a Skin-Friction Gage to a Local Mach Number of 4.9. NASA TN D-3830, 1967.

9. Lamb, Milton; Stallings, Robert L., Jr.; and Richardson, Celia S.: Aerodynamic Characteristics of 1/25-Scale Model of YF-12 Airplane at Mach 1.80 to 2.96 With and Without External Instrument Packages and Flow-Field Surveys at Mach 2.96. NASA TM X-2524, 1972.

10. Peterson, John B., Jr.: Boundary-Layer Velocity Profiles Down Stream of Three-Dimensional Transition Trips on a Flat Plate at Mach 3 and 4. NASA TN D-5523, 1969.

11. Winter, K. G.: An Outline of the Techniques Available for the Measurement of Skin Friction in Turbulent Boundary Layers. Tech. Memo. Aero., 1956, Royal Aircraft Establishment, 1975.

12. Coles, Donald: Measurements in the Boundary Layer on a Smooth Flat Plate in Supersonic Flow. Part I. The Problem of a Turbulent Boundary Layer, Rept. 20-69, Jet Propulsion Lab., Calif. Inst. of Technology, June 1953.

13. van Driest, E. R: Turbulent Boundary Layer in Compressible Fluids. IAS J., vol. 18, no. 3, Mar. 1951, pp. 145-160, 216.

14. Eckert, Ernest R. G.: Survey of Boundary Layer Heat Transfer at High Velocities and High Temperatures. WADC Tech. Rep. 59-624, Wright Air Dev. Center, U.S. Air Force, Apr. 1960. (Available from ASTIA as 238292.)

15. Keener, Earl R.; and Hopkins, Edward J.: Turbulent Boundary-Layer Velocity Profiles on a Nonadiabatic Flat Plate at Mach Number 6.5. NASA TN D-6907, 1972.

16. van Driest, E. R.: The Problem of Aerodynamic Heating. Aero. Eng. Rev., vol. 15, no. 10, Oct. 1956, pp. 26-41.

17. Spalding, D. B.; and Chi, S. W.: The Drag of a Compressible Turbulent Boundary Layer on a Smooth Flat Plate With and Without Heat Transfer. J. Fluid Mech., vol. 18, part I, Jan. 1964, pp. 117-143.

18. Cary, Aubrey M., Jr.: Summary of Available Information on Reynolds Analogy for Zero-Pressure-Gradient, Compressible, Turbulent-Boundary-Layer Flow. NASA TN D-5560, 1970.

TABLE 1.—FREE STREAM CONDITIONS

Flight	M_∞	P_∞, N/m^2	T_∞, K	α, wing, deg	β, deg	Re_∞/m, per m
A	3.02	4178	218	3.9	0	4.28×10^6
B	2.98	4092	217	3.8	0	4.07×10^6

TABLE 2.—LOCAL (CYLINDER) CONDITIONS

Flight	M_δ	T_w/T_R	P_δ, N/m^2	T_δ, K	α, deg	β, deg	Re_δ/m, per m	Re_θ
A	2.90	0.91	4943	229	0 ± 0.05	0 ± 0.10	4.49×10^6	8664
B	2.92	0.66 to 0.77	4413	222	0 ± 0.05	0 ± 0.10	4.17×10^6	---[a]

[a] Boundary-layer velocity profiles were not obtained during flight B. Consequently, the experimental momentum thickness Reynolds number was not available for this flight; however, sufficient data were obtained from the pitot pressure rake to determine the boundary-edge Mach number.

TABLE 3.—BOUNDARY LAYER MACH NUMBER AND VELOCITY DISTRIBUTIONS

Flight A

x = 274 cm; θ = 0.193 cm; M_δ = 2.90;

T_δ = 229 K; U_δ = 880 m/sec; P_δ = 4943 N/m^2; δ = 3.05 cm

y, cm	$\frac{y}{\delta}$	$\frac{M}{M_\delta}$	$\frac{T}{T_\delta}$	$\frac{U}{U_\delta}$
0.254	0.083	0.566	1.64	0.724
0.432	0.142	0.617	1.55	0.769
0.610	0.200	0.66[illegible]	1.46	0.805
0.787	0.258	0.700	1.41	0.833
0.965	0.316	0.734	1.36	0.857
1.321	0.433	0.797	1.27	0.896
1.956	0.641	0.903	1.12	0.956
2.591	0.849	0.979	1.02	0.990
3.226	1.058	1.000	1.00	1.000
3.861	1.266	1.003	1.00	1.003
4.496	1.474	1.003	1.00	1.003

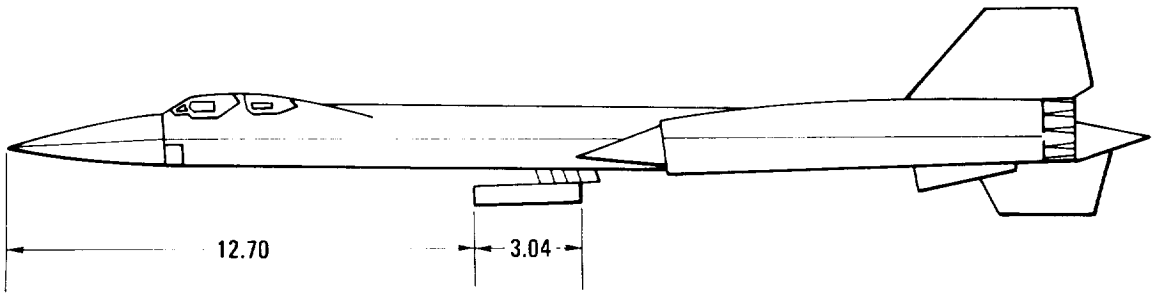

Figure 1.—YF-12A airplane showing location of hollow cylinder. Dimensions in meters.

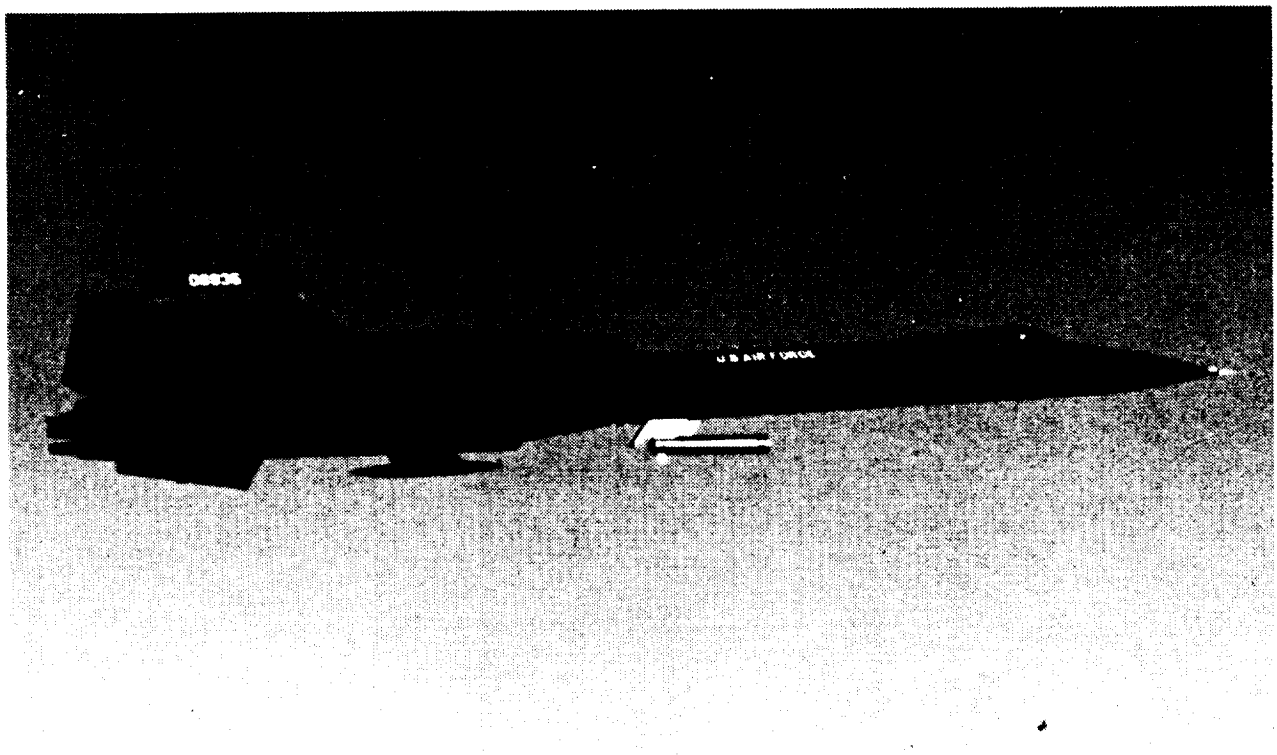

Figure 2.—YF-12A airplane with hollow cylinder attached.

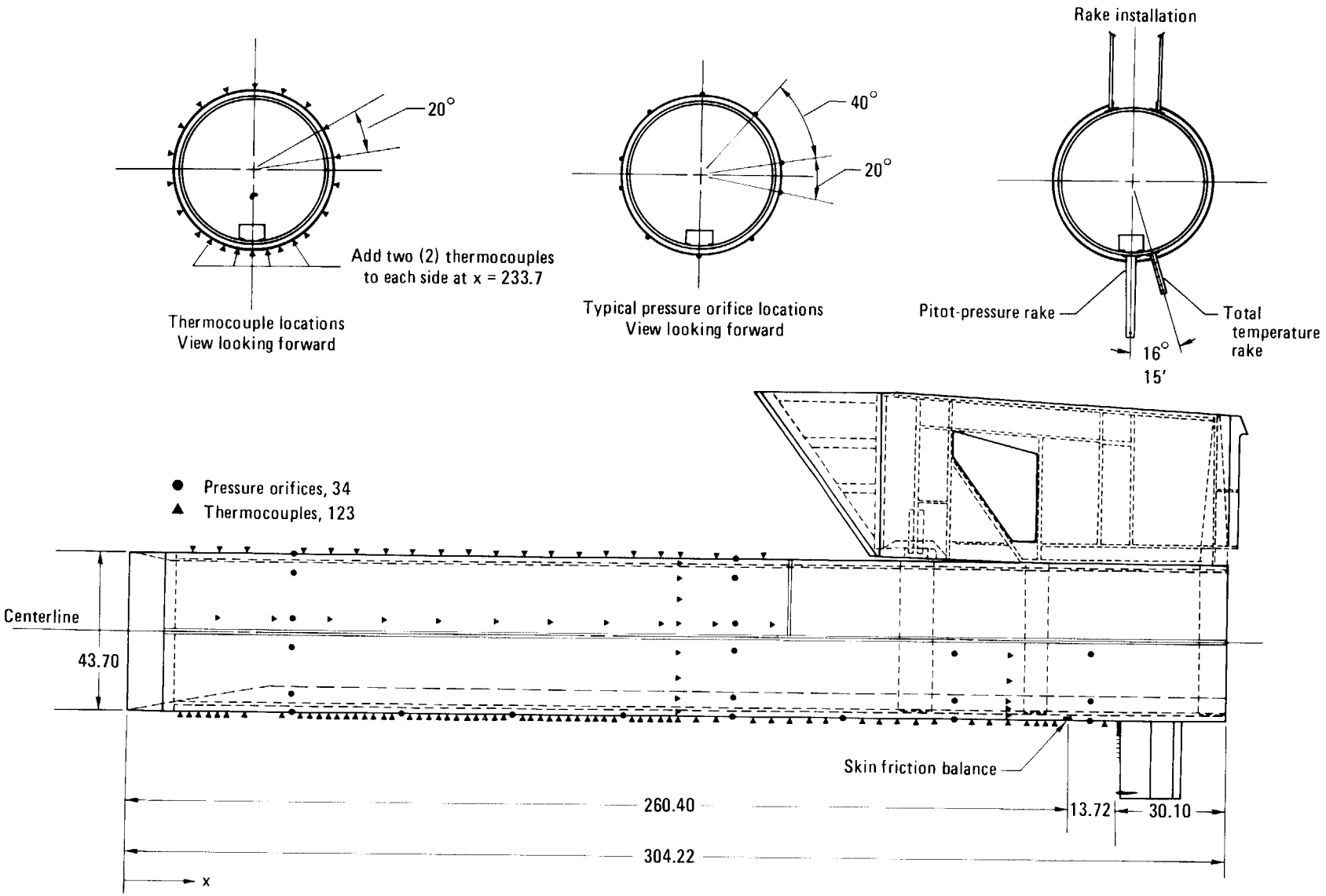

Figure 3.—Location of instrumentation on hollow cylinder. Dimensions in centimeters.

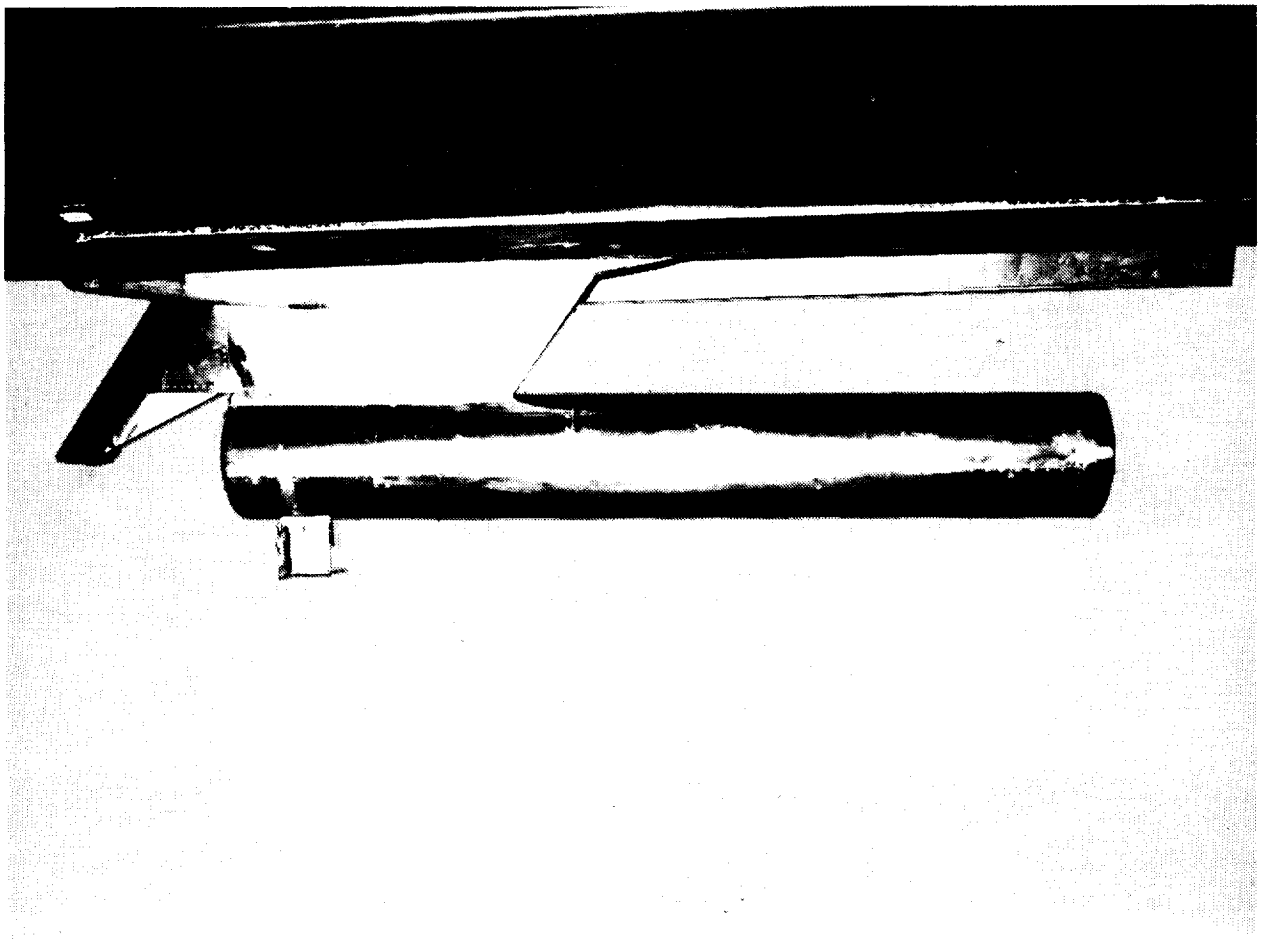

Figure 4.—Hollow cylinder (flight A).

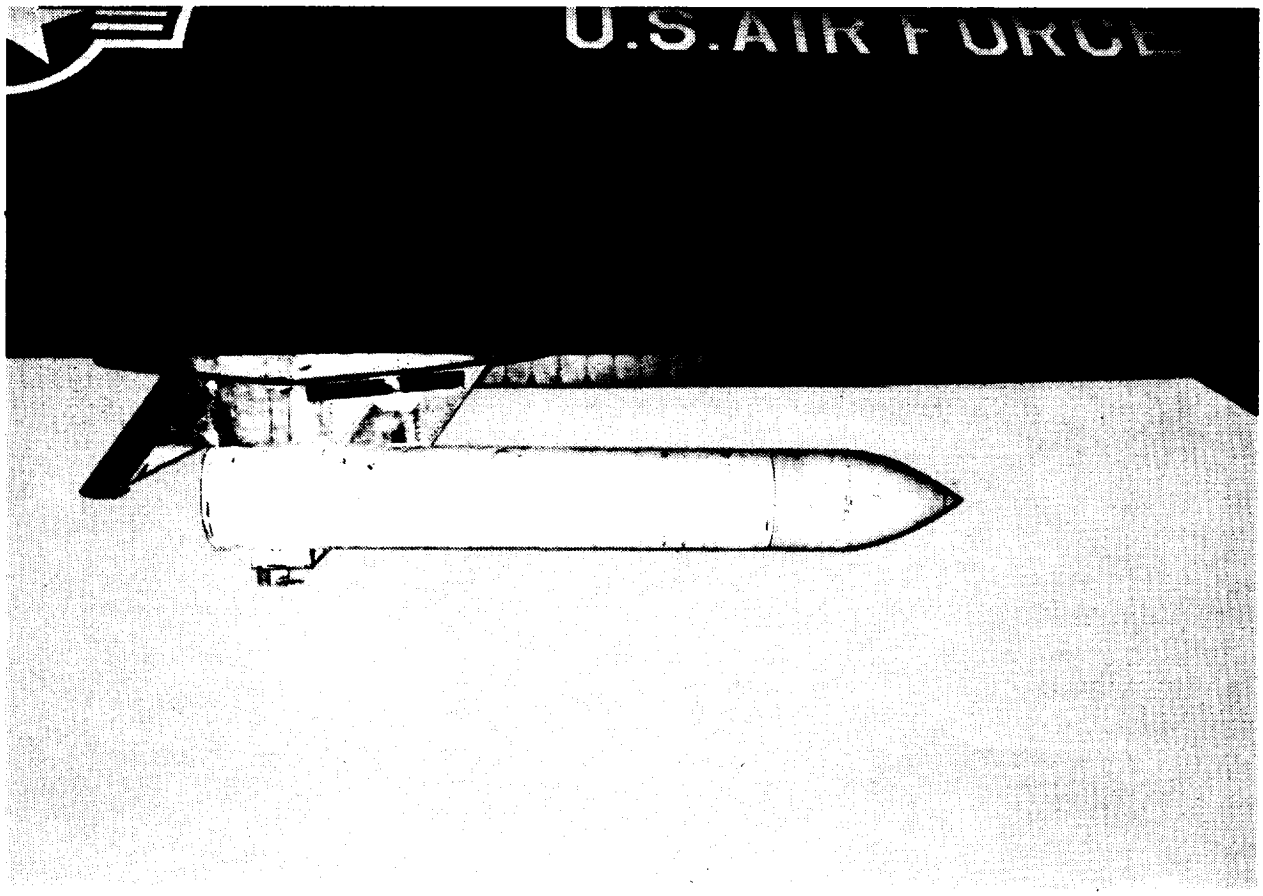

Figure 5.—Hollow cylinder with insulating cover (flight B).

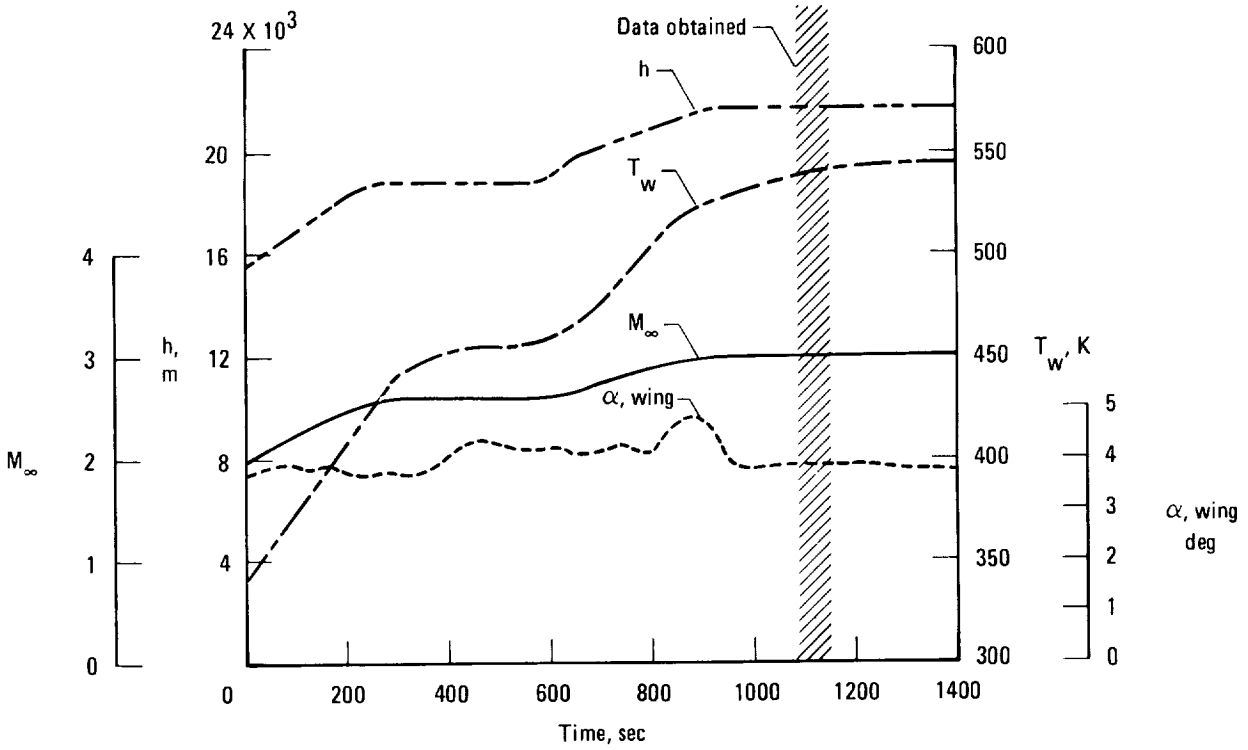

(a) Flight A.

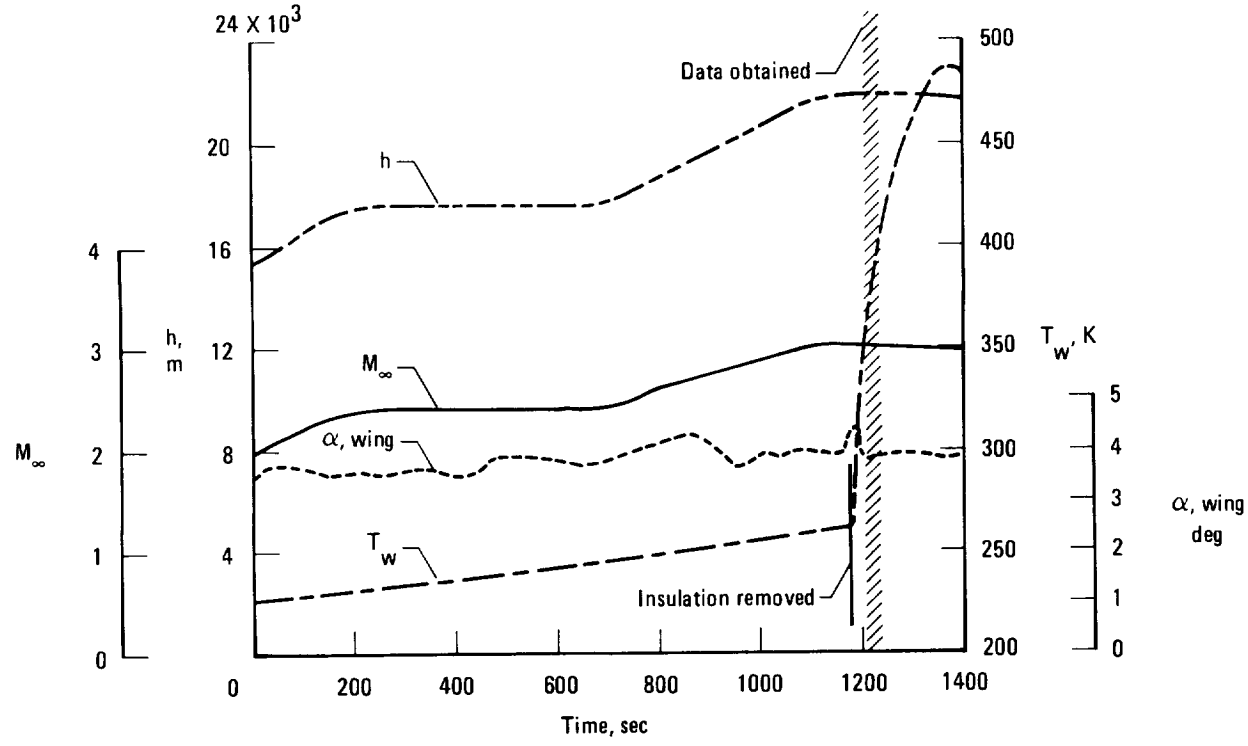

(b) Flight B.

Figure 6.—Time history of flight parameters and typical skin temperatures.

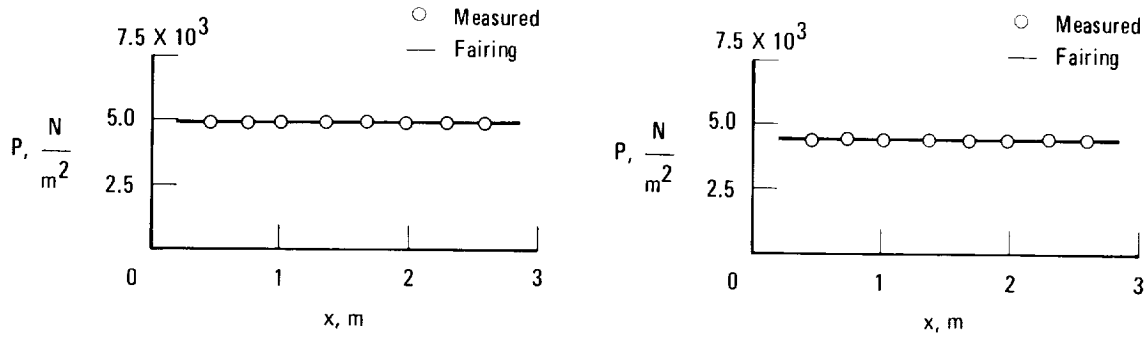

(a) Flight A.

(b) Flight B.

Figure 7.—Surface static pressures measured on the lower cylinder centerline.

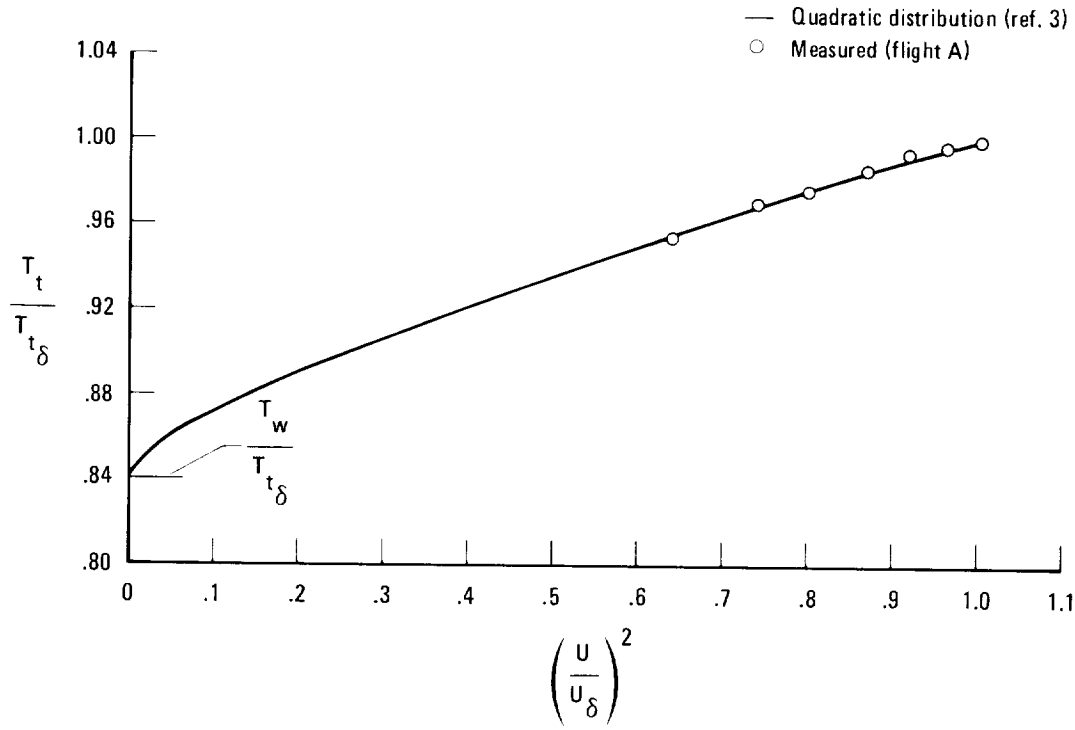

Figure 8.—Comparison of theoretical and measured boundary layer total temperature ratios.

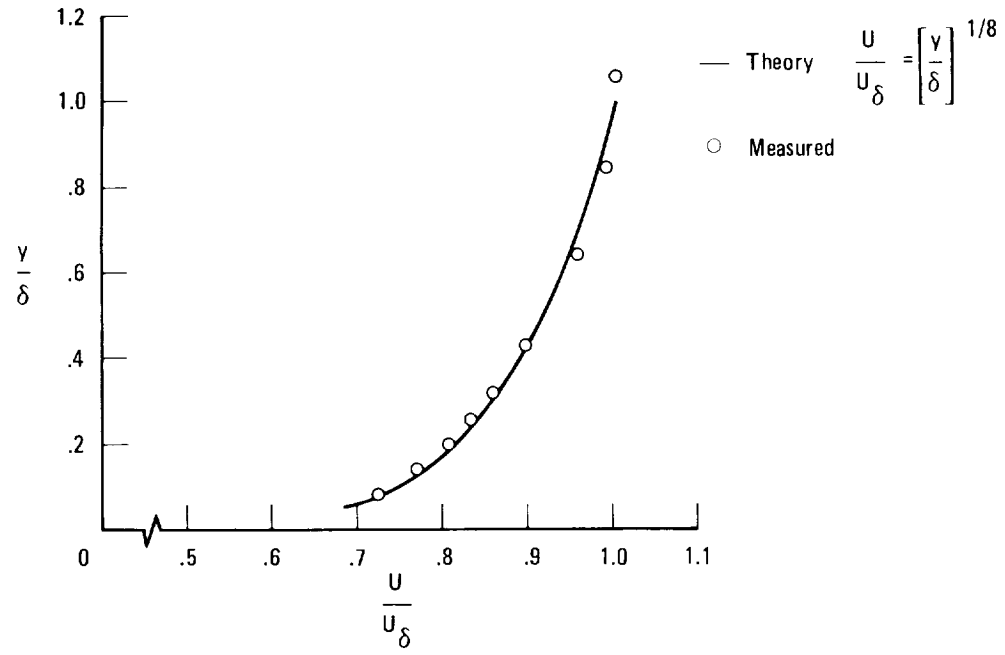

Figure 9.—Boundary layer velocity profile for flight A. $M_\delta = 2.90$, $Re_\theta = 8664$, $\delta = 3.05$ cm.

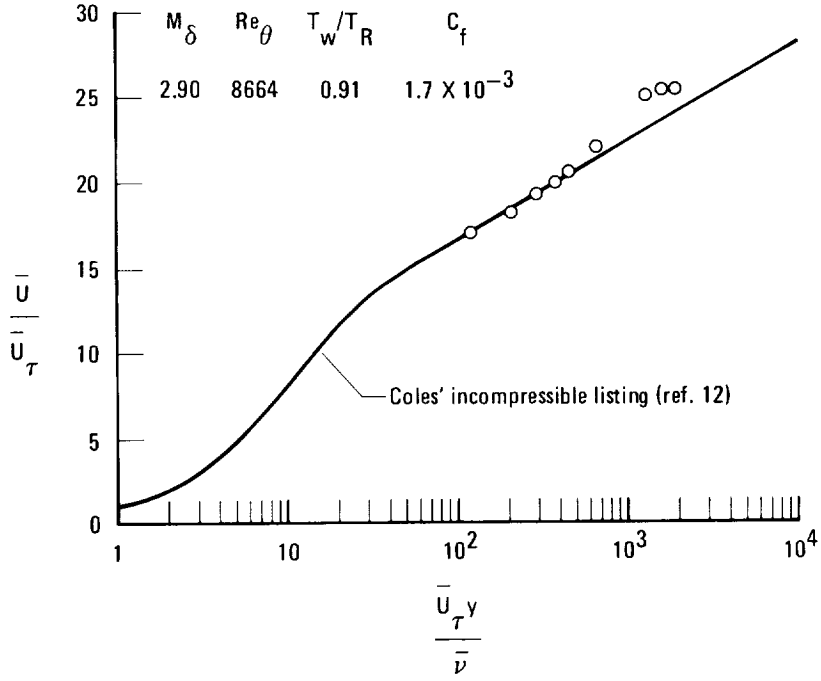

(a) Mixing length transformation of van Driest.

Figure 10.—Law-of-the-wall velocity profiles for flight A.

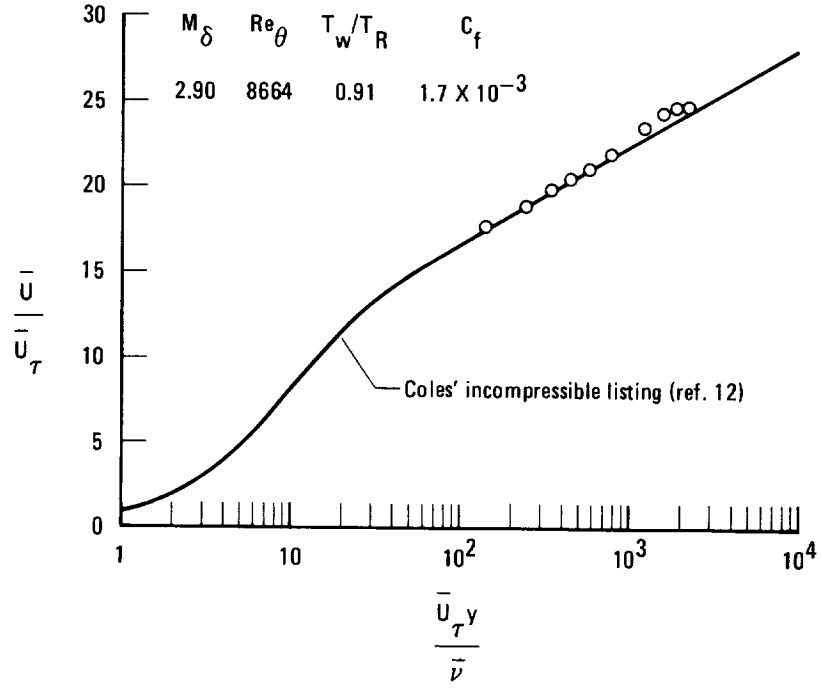

(b) Eckert's reference enthalpy transformation.

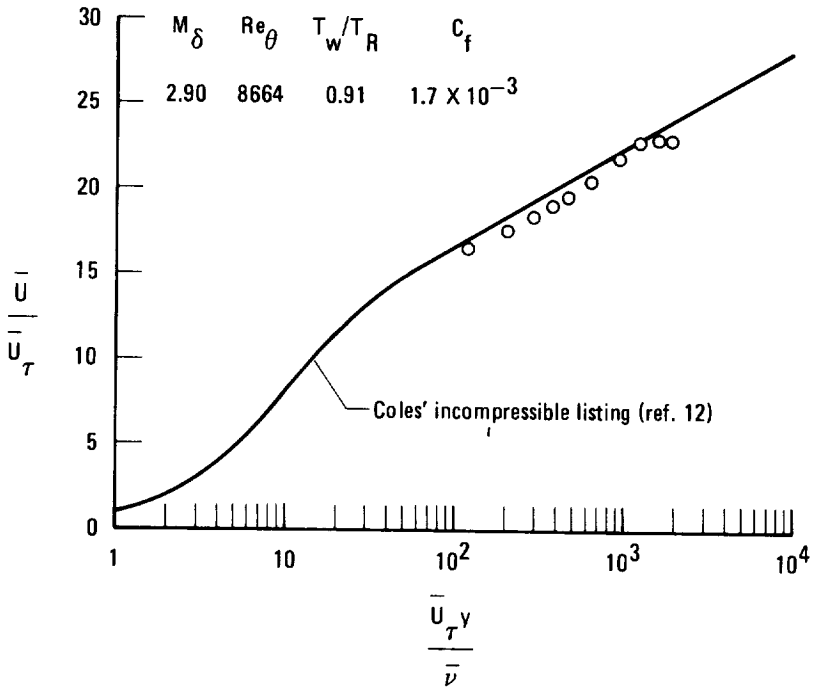

(c) Wall reference temperature transformation.

Figure 10.—Concluded.

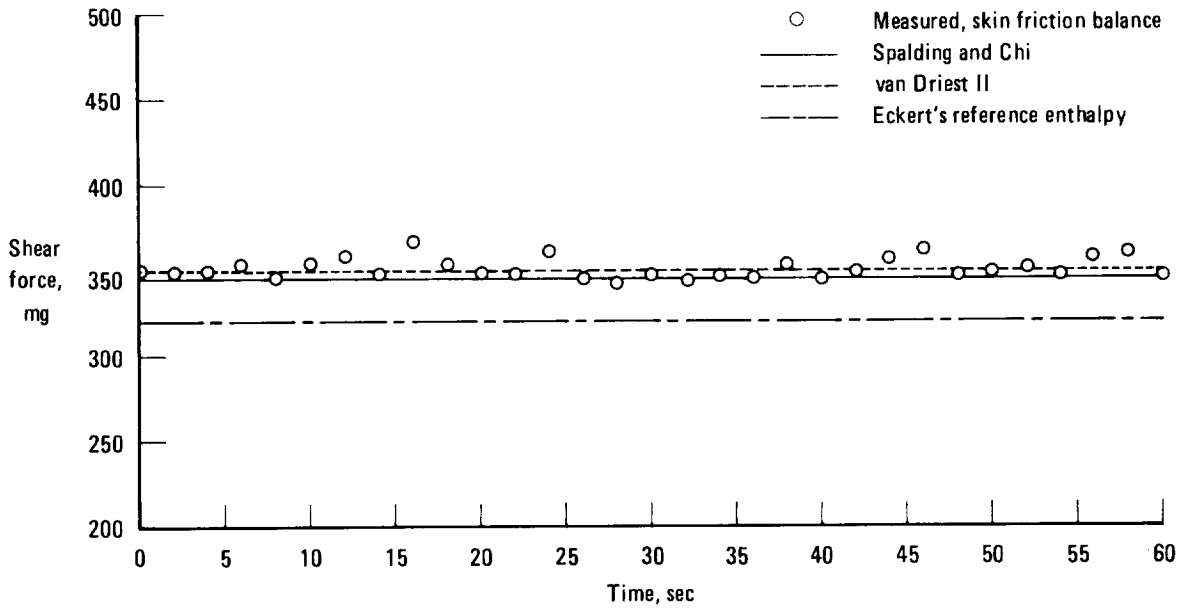

Figure 11.—Comparison of measured and calculated skin friction for flight A. $M_\delta = 2.90$, $Re_\theta = 8664$, $T_w/T_R = 0.91$.

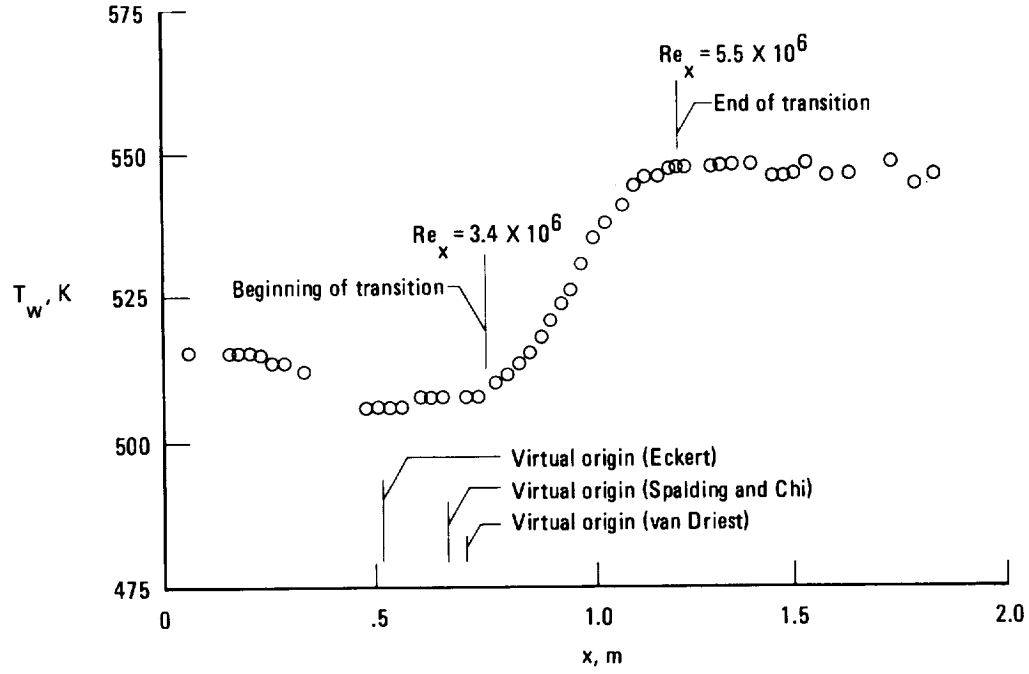

Figure 12.—Boundary layer transition on lower surface for flight A.

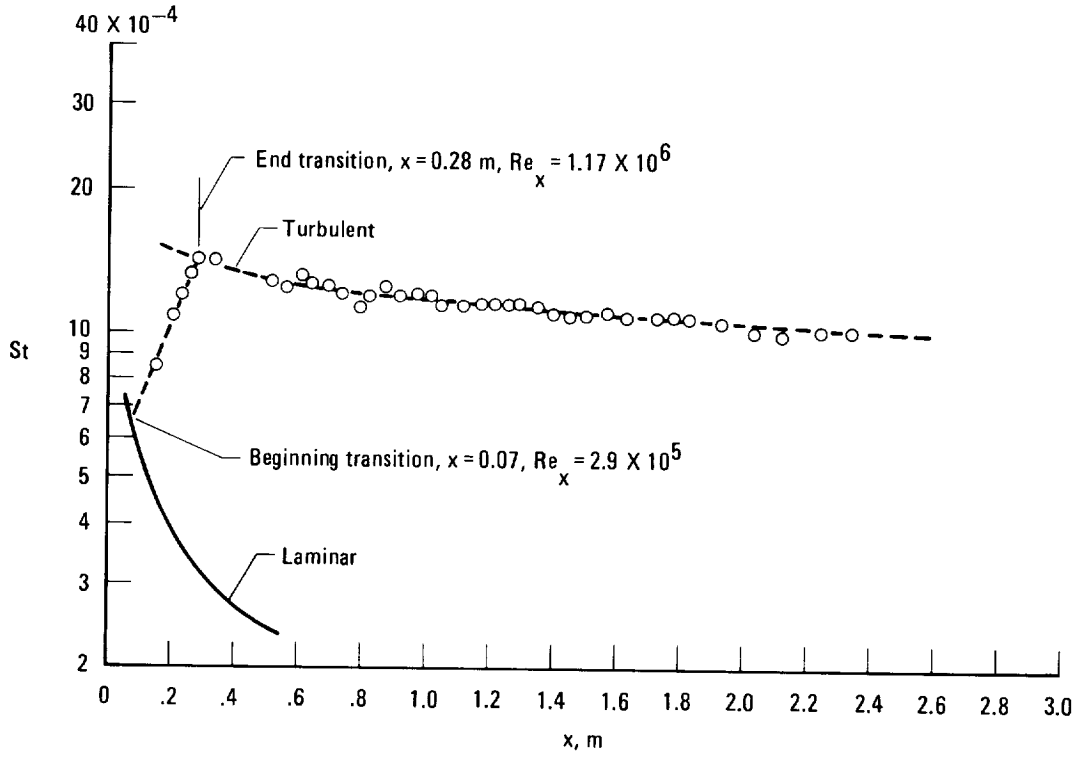

Figure 13.—Boundary layer transition on lower surface for flight B.

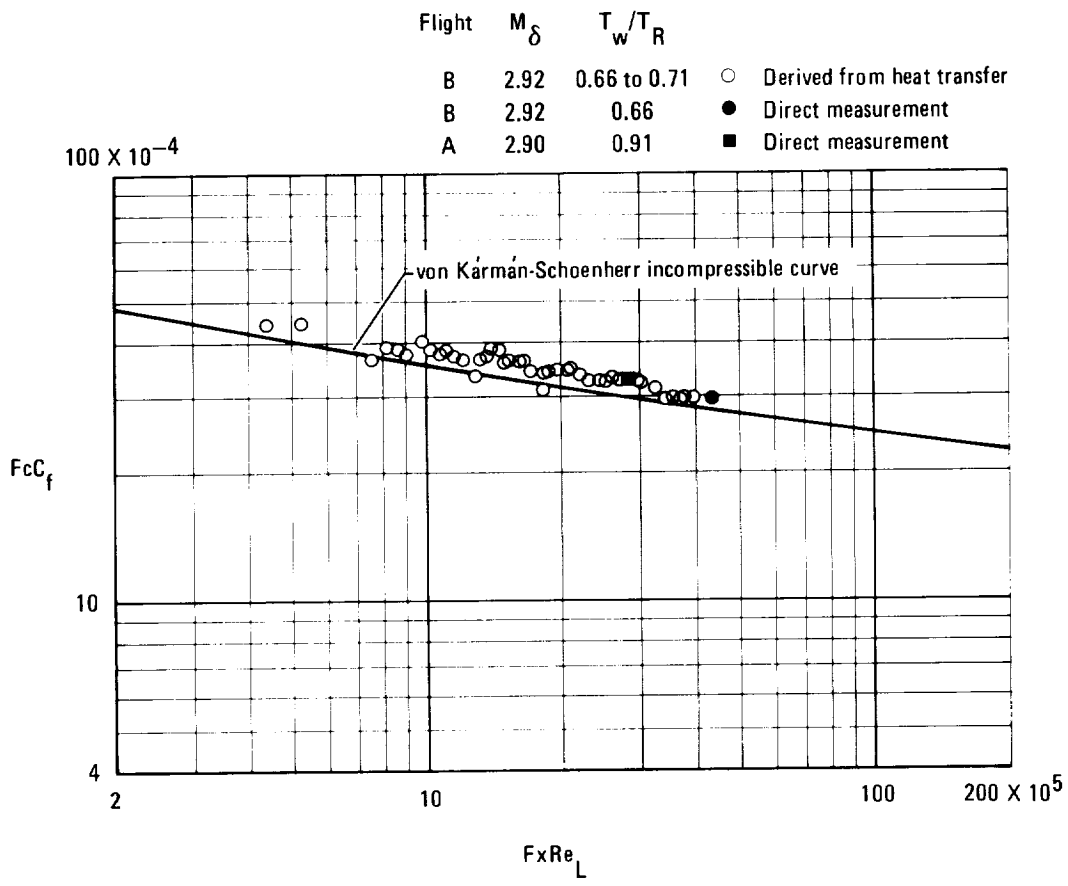

(a) Eckert's reference enthalpy.

Figure 14.—Evaluation of three compressible turbulent skin friction theories.

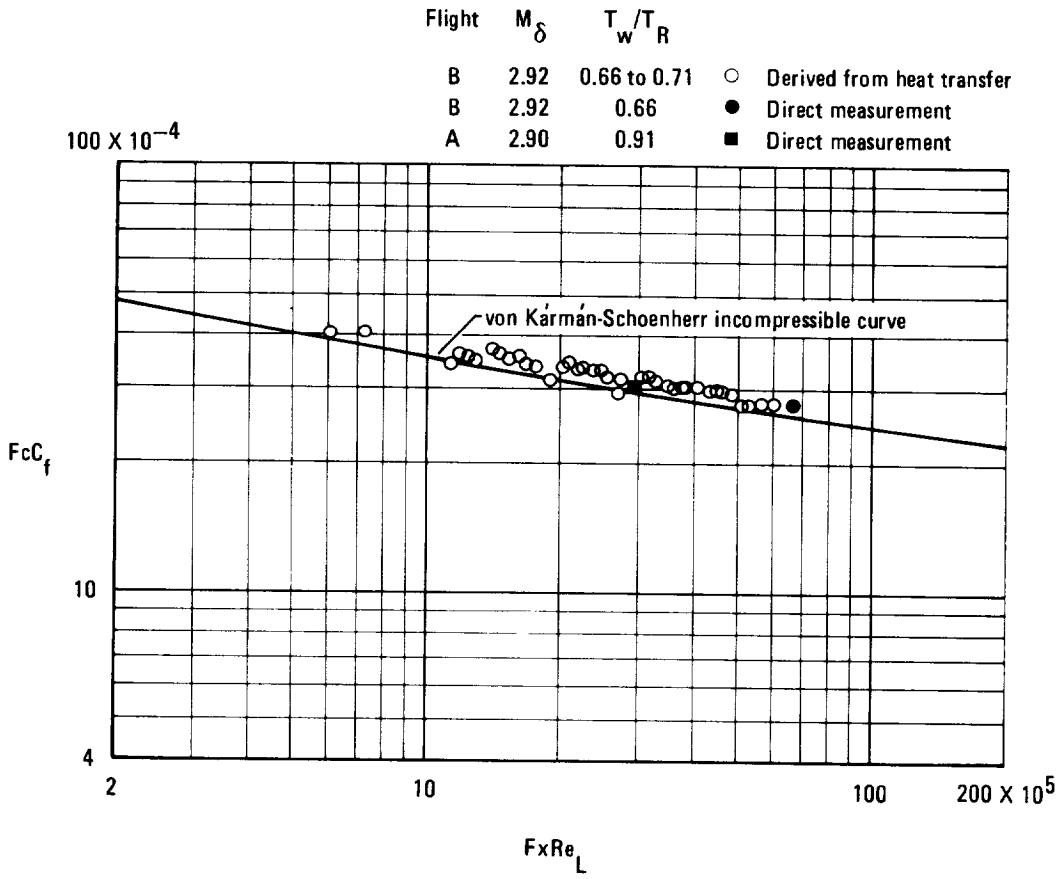

(b) Spaulding and Chi.

Figure 14.—Continued.

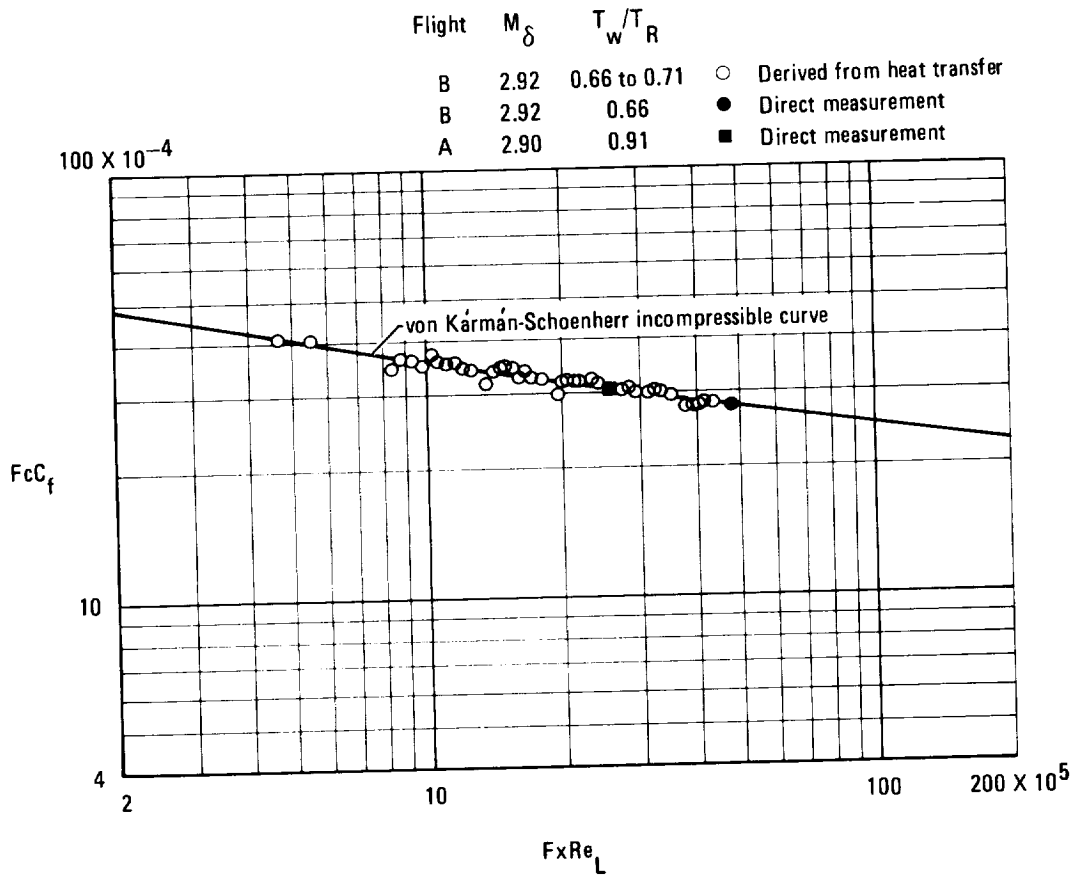

(c) van Driest II.

Figure 14.—Concluded.

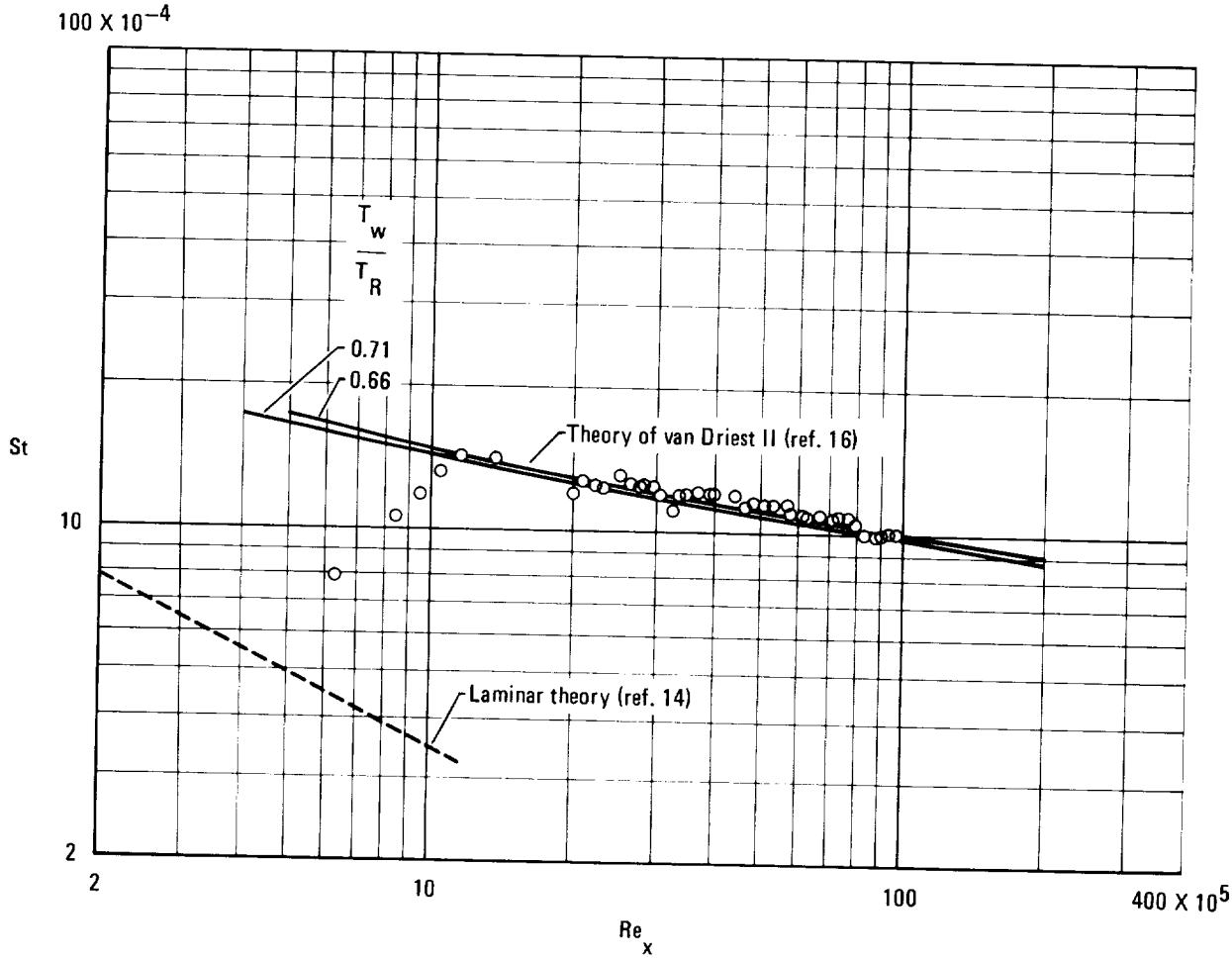

Figure 15.—Comparison of measured and calculated heat transfer for flight B.